Proceedings of ASME/JSME:
Joint Fluids Engineering Conference
July 18-22, 1999, San Francisco, California

FEDSME99-6930

# The simulation and interpretation of turbulence with a cognitive neural system

**Francesc Giralt**
Departament d'Enginyeria Química
Universitat Rovira i Virgili
Carretera de Salou s/n, 43006 Tarragona
Catalunya, Spain

**Alex Arenas**
Departament d'Enginyeria Informàtica
Universitat Rovira i Virgili
Carretera de Salou s/n, 43006 Tarragona
Catalunya, Spain

**Joan Ferre-Giné**
Departament d'Enginyeria Informàtica
Universitat Rovira i Virgili
Carretera de Salou s/n, 43006 Tarragona
Catalunya, Spain

**Robert Rallo**
Departament d'Enginyeria Informàtica
Universitat Rovira i Virgili
Carretera de Salou s/n, 43006 Tarragona
Catalunya, Spain

## ABSTRACT

A neural network based on fuzzy ARTMAP that is capable of learning the basic non-linear dynamics of a turbulent velocity field is presented. The neural system is capable of generating a detailed multi-point time record with the same structural characteristics and basic statistics as those of the original instantaneous velocity field used for training. The good performance of the proposed architecture is demonstrated by the generation of synthetic two-dimensional velocity data at eight different positions along the homogeneous (spanwise) direction in the far region of a turbulent wake flow generated behind a cylinder at (Re=1,200) and (x/D=420). The analysis of the synthetic velocity field, carried out with spectral techniques, POD and pattern recognition, reveals that the proposed neural system is capable of capturing the highly non-linear dynamics of free turbulence and of reproducing the sequence of individual classes of relevant events present in turbulent wake flows. The trained neural system also yields patterns of the coherent structures embedded in the flow when presented with input data containing partial information of the instantaneous velocity maps of these events. This feature could be used to help in the interpretation of turbulent data measured in complex fluid flow experiments or obtained by direct numerical simulation.

## INTRODUCTION

Turbulence is a fluid flow phenomenon of significant fundamental interest as well as of commercial importance for its impact in the operational performance and costs of many industrial processes and of transportation systems. It is characterized by an irregular space and time dependence of the velocity and scalar fields which is the result of vortical three-dimensional motions that occur at high Reynolds numbers, when the ratio of inertial to viscous forces is high (Townsend, 1976; McComb, 1990). The study of turbulent flows relies heavily on experimental data and on the numerical solution of the Navier-Stokes equations of fluid motion because turbulence is an unsolved classical problem (Nelkin, 1992). The interpretation and control of the very large range of excited space and time scales present in these flows, and of the associated mixing that they cause (Kadanoff, 1996), requires the application of analytical, experimental and computational techniques (Sreenivasan, 1990).

Flow visualizations carried out by Brown and Roshko (1974) and Falco (1977) showed that there are large-scale, recurrent, coherent eddies among the vortical motions present in turbulent flows. A large number of quantitative techniques, such as spatial correlation functions and POD (Grant, 1958; Lumley, 1965; Adrian and Moin, 1988), pattern recognition and conditional averaging





ISBN 0-7918-1961-2

(Townsend, 1979; Antonia, 1981; Ferre and Giralt, 1989; Ferre-Gine et al., 1996; Kopp et al., 1997), etc., have been developed to determine the structure of turbulent fields. These techniques use features of the coherent motions to identify and educe them from measured or numerical data sets, in a closed, non-interactive mode. It is interesting to note that the fuzzy-neural network pattern recognition technique developed by Ferre-Gine et al. (1996) could operate as an automatic, free from operator bias, classification technique capable of categorizing all types of coherent and disordered motions present in the data. This capability could be exploited to generate turbulent signals if the method could be reversed, i.e., could predict a sequence of classes of patterns from an initial velocity condition. Could, thus, such a neural network be used not only to classify events but also to capture and reproduce the dynamics of their occurrence? Could this system be applied openly and interactively to identify the structure present in any turbulent flow as an expert system?

Here we report a cognitive neural network architecture based on fuzzy ARTMAP (Carpenter et al., 1992) that is capable of learning the basic non-linear dynamics of a turbulent velocity field and to generate, afterwards, a detailed multi-point time record as detailed as can be measured in a laboratory experiment. The problem dealt with in the present study at the simulation stage is not that of exactly forecasting the measured field but that of generating turbulence after learning the basic statistics and structural characteristics from historic examples of the original (Denker et al., 1987; Seung et al., 1992). At the interpretation or expert system stage, the trained neural system is used to determine the existence and topology of coherent structures that could be present in the flow field investigated, by generating sequences of data from inputs containing partial information of the velocity field of the investigated structure. The flow analyzed is a fully developed turbulent wake generated behind a circular cylinder.

## THE NEURAL SYSTEM

**Background and network requirements.** An artificial neural network is a modeling and computational technique, based on the observed behavior of biological neurons, which is used to mimic the performance or simulate the dynamics of a system from examples. In some cases these networks are used in combination with the theory of fuzzy logic systems so that in addition to learn from experience, to carry out tasks faster, with less computer space requirements, they accept both numerical data and fuzzy commands as inputs. Fuzzy and neural systems or a combination of the corresponding logic and network architectures have been applied to identify, classify, control, forecast, predict, diagnose, model, design and analyze events in several fluid-base systems of interest to medicine, vehicle and transportation systems, aerospace, manufacturing, meteorology, mining, etc. (Tzes and Borowiec, 1996). Examples of fluid-base applications in engineering include the reduction of drag, the minimization of energy consumption or losses, the prediction of transport rates in industrial equipment, the reduction of noise, and phenomena related to pressure dynamics.

A significant portion of the above mentioned applications are related to flow turbulence and arise from the need to control some aspects of this highly non-linear phenomenon. Thus, the performance of a neural system in these applications could be evaluated by its ability to learn the dynamics of turbulence in some pre-selected regions of the flow field. Feedforward, feedback and other standard architectures are capable of capturing some aspects of the dynamics of turbulent flows. For example, Lee et al. (1997) have established the correlation between some near-wall turbulence parameters and the wall actuation needed to reduce drag. However, it remains to be determined whether these or other architectures are capable of first learning and then simulating in a global sense flow turbulence.

One indispensable requirement for attempting the simulation of a synthetic turbulent velocity field, i.e., of simultaneous multi-point turbulent velocity time-records, with a neural network is that the architecture should be capable to learn and to generate the irregular time-sequences of velocity patterns associated with turbulence. This requires that the artificial neural system should be able to select, in an automated way, a path in this complex sequence of real events or patterns on the basis of past experience and, therefore, should have the following characteristics:

(i) Powerful in difficult classification problems.

(ii) Capable of generalizing the information with an efficient mechanism for resetting patterns and creating new categories, avoiding the stability-plasticity dilemma (Carpenter and Grossberg, 1987; Carpenter et al., 1991a, 1991b, 1992), i.e., the dilemma of either hindering stability by activating endlessly new categories in competitive learning or losing the plasticity or ability of the network to react to any new data because the learning rate is gradually reduced to zero. This characteristic of the Adaptive Resonance Theory (ART) is important in the real time learning of systems that are continuously adapting in a non-stationary situation. The more popular feedforward and feedback architectures present the difficulty of establishing the sufficient dimension of the system or number of neurons that is required for the network to exhibit long memory span capabilities. A pertinent discussion on the long memory span requirements to resolve ambiguities in forecasting problems can be found in Kühn et al. (1989).

(iii) Associative memory or memory organization accessed by its content, with a sufficiently long memory span to resolve the ambiguities in the succession states that characterize the dynamics of highly non-linear systems. The architecture should remember by retrieving previously stored information in response to associated data.

(iv) Fuzzy rules in the learning algorithm since they are especially adequate for the treatment of real data (Kosko, 1992).

One convenient an automated way to select a path in this complex sequence of real events or patterns on the basis of past experience is the implementation of a cognitive neural system with fuzzy rules in the learning algorithm. One reasonable choice is the Fuzzy ARTMAP neural system.

**Architecture.** The Fuzzy ARTMAP neural network is formed by a pair of fuzzy ART modules, Art_a and Art_b, linked by an associative memory and an internal controller (Carpenter et al., 1992), as shown in Fig. 1 but with the output disconnected. The Fuzzy ART architecture was designed by Carperter et al. (1991b) as a classifier for multidimensional data clustering based on a set of features. The elements of the set of n-dimensional data vectors $\{\xi^1,..., \xi^p\}$, where $p$ is the number of vectors to be classified, must be interpreted as a pattern of values showing the extend to which each feature is present.

Every pattern must be normalized to satisfy the following conditions:

$$\xi^i \in [0,1]^n$$
$$\sum_{j=1}^{n} \xi_j^i = k \qquad \forall i = 1,...,p \tag{1}$$

The classification procedure of fuzzy ART is based on *Fuzzy Set Theory* (Zadeh, 1965). The similarity between two vectors can be established by the grade of the membership function, which for two generic vectors ($l$, $m$) can be easily calculated as

$$\text{grade}(\xi^l \subset \xi^m) = \frac{\left|\xi^l \wedge \xi^m\right|}{\left|\xi^l\right|} \tag{2}$$

In this equation (2) the fuzzy AND operator $\wedge$ is defined by,

$$\wedge : [0,1]^n \times [0,1]^n \rightarrow [0,1]^n$$

and the components of the image vector that results from this application are

$$\xi_j^i = \min\left(\xi_j^l, \xi_j^m\right) \quad \forall j = 1..n \tag{3}$$

The norm $|\bullet|$ in equation (2) is the sum of the components of the vector defined by equation (3).

The classification algorithm clusters the data that have a value of (2) greater than the *vigilance parameter* $\rho$ into groups or classes. The value of $\rho$ controls the granularity of the classes and allows the implementation of a desired accuracy criteria in the classification procedure. Each class $\mu$ is represented by a vector $\omega^\mu$ named weight vector. The procedure starts by creating the first class from the first pattern presented to the network,

$$\omega^1 = \xi^1 \tag{4}$$

The rest of input patterns $\xi^i$ (i=2,...,p) are presented to the network and if the similarity of $\xi^i$ with any established class $\mu$ is greater than $\rho$ then $\xi^i$ is classified into this class, and the representative of this class is updated according to

$$\omega_{new}^\mu = \omega_{old}^\mu \wedge \xi^i \tag{5}$$

Otherwise a new class represented by $\xi^i$ is created. Equation (5) is the learning rule of the net. The mechanisms to speed up the process and to conduct the classification properly can be found elsewhere (Carpenter et al., 1991b).

The dynamics of Fuzzy ARTMAP is essentially the same as two separate Fuzzy ART networks, each one working with a part of the training vector; the first part could be interpreted as the input pattern and the second one as the desired classification output (supervisor). The associative memory records the link between the classes corresponding to the input pattern and the desired classification. The internal controller is the responsible of supervising if a new link is in contradiction with any other previously recorded. If no contradiction is found, the link is recorded, but in the case of a contradiction, the pattern is re-classified with a larger vigilance parameter. Once the network has been trained it can be used to classify input vectors without any additional information.

The Fuzzy ARTMAP architecture, which has been successfully applied to educe the different classes of large scale events present in free turbulence (Ferre-Gine et al., 1996), was designed to classify data and, thus, cannot generate an output pattern after the training stage. To implement this new mode of operation the categories educed by the system from the learned information are linked to the desired outputs, as depicted in Fig. 1. This is mathematically equivalent to defining an application from the space of categories to that of output patterns, the image of the application being defined by examples of patterns provided to the neural system in a supervised manner. The accuracy of the procedure increases asymptotically towards a constant value with the number of examples used for training, i.e., when the space of outputs is accurately mapped. In the predictive mode, only the category layer of Art_b in Fig. 1 is active and linked to Art _a to provide an output for each input vector presented to this module.

**Experimental Data and Training Sets.** The performance of the proposed neural system has been evaluated by simulating the two-dimensional velocity field measured at eight different positions (k = 1, 2,..., 8) along the homogeneous (spanwise) direction of a turbulent wake flow generated behind a cylinder at *Re=1200* and *x/D=420*. The freestream velocity of this flow was $U_0$=6.7 m/s and the cylinder diameter $D$=2.67 mm. The structural characteristics of these fully developed turbulent wake data, provided by R.A. Antonia (University of Newcastle), have been previously examined by Kopp et al., (1997) using pattern recognition and proper orthogonal decomposition (POD). Fig. 2 illustrates the experimental flow configuration for the case where the (u, w) velocity data used to train the net were measured with eight X-wire anemometric probes located along the homogeneous spanwise direction at the half width of the wake ($l_0$=12.3 mm), i.e., at the vertical position where the mean velocity defect is half the maximum value. The eight sensors spanned approximately 2.87$l_0$ in the z-direction. The voltage signals were sampled at 2717 Hz for 30 s. A sample of the experimental data (u, w) is included in Fig. 3 to visualize the irregularity of the individual time-records and the instantaneous velocity map of the projected velocity field in the horizontal plane. The validity of Taylor hypothesis in the far wake region, where turbulence is nearly frozen, allows the conversion of

time into the streamwise coordinate, $x = U_0 t$, and the analysis of data in the time-sequence in terms of the streamwise x-direction.

The neural system proposed was formed by eight Fuzzy ARTMAP networks like the one shown in Fig. 1. These networks were working in parallel and synchronously, one for each experimental device measuring simultaneously the two-component velocity signals u and w at a given k-location in the wake flow. Each individual network was first trained with the output in Fig. 1 disconnected. The training data for each individual network consisted of vectors with 12 elements - four temporal or historical and two spatially adjacent values for each velocity component u and w - for the Art_a module, and of vectors with two elements - the following value of each velocity component in the time sequence - for the Art_b module. Thus, simultaneous space-time information was provided to the neural system in terms of the input to each Art_a module, with the corresponding future information for (u, w) given to each Art_b module, with no other association between individual networks. At the two extreme locations (k = 1 and 8) the spatial information was provided from the one-sided contiguous locations (k+1, k+2) and (k-1, k-2), respectively.

The dimension of the input vectors to the eight neural networks and the type of simultaneous space-time information that they contained was decided after examination of the space-time correlation of the experimental data, so that relevant structural characteristics of the flow were provided to the system during training. The choice of considering four temporal data for each velocity component in the training input vectors is consistent with the Takens theorem (Takens, 1981), which states that good accuracy can be achieved in a point-to-point forecasting in a system with attractors of dimension d when a function that depends at most on (2d+1) past measurements is used. For the wake flow this implies using between four and five historical data in the training sets.

The system was trained using the first 2000 instants of the experimental velocity field (u, w). This was sufficient to match the local fractal dimension of 1.75± 0.02 and 1.78±0.02 of the simulated u and w signals, respectively, with the values 1.76±0.02 and 1.78±0.02 of the experimental data. The local fractal dimension was calculated by the box-counting dimension procedure described by Scotti et al. (1995). Additional training tests with up to 40,000 samples yielded comparable statistics but improved structural characterization, as is discussed in the next Section. A non-optimized version of the code required less than 1 hour of total CPU time for training in a Sun Ultra 2250 workstation.

After training, instants( 2001-2004) of measured u and w at each location were used together with the two spatial data of the instant 2004 as the initial input vector to the Art_a module of each net. The output (u, w) for the instant 2005 was generated by each Art_b module with only the categories layer and the output activated. The output calculated by each network was added to the corresponding data sequence and a new input pattern was formed with historicals (2002-2005) and with the two spatial data predicted simultaneously by the two neighboring networks also at instant 2005. Such operation of the neural system produced a two-component velocity field of eight velocity data pairs (u, w) every 0.14 seconds of CPU with the two processors of the workstation working in parallel.

## SIMULATION OF FREE TURBULENCE

To evaluate the performance of the proposed network architecture 81,600 time instants or 29.4s of (u,w) velocity signals were generated at time intervals of $\Delta t$=0.368ms. No repetitions in the predicted velocity field were observed over this time-period. The (u,w) results obtained in the homogeneous x-z plane of the wake are evaluated in detail in this section using basic statistics, spectral and correlation analysis, POD and pattern recognition. The preliminary evaluation of the performance of the proposed neural system for non-homogeneous turbulence (x-y plane) is also reported. All space variables are normalized with respect to $l_0$ as

$$x^* = \frac{\Delta x}{l_0} \cong \frac{U_0 \Delta t}{l_0}, \; y^* = \frac{\Delta y}{l_0}, \; z^* = \frac{\Delta z}{l_0}$$

The flow in all vector maps is from left to right. The statistics of the two-dimensional instantaneous turbulent velocity field (u, w) measured and simulated by the present architecture with training sets of 2,000 and 24,000 samples, respectively identified as ANN-2000 and ANN-24000, are given in Table 1. The comparison of the statistics of the two predicted time records shows that training with 2,000 instants of data is sufficient to capture the irregularity of the time sequence, as is also the case for the local fractal dimension. Thus, the results analyzed in this section correspond mostly to ANN-2000. The mean of the predicted velocity field reported in Table 1 deviates a maximum of 0.2%, in terms of the free stream velocity, from the zero mean experimental fluctuating field. The rms values of the fluctuating field generated for u and w are also in agreement with experimental data, with a maximum deviation of 9.2%. The Reynolds shear stress field is equal to zero, within the limits of the experimental error of the data, as should be the case in the homogeneous spanwise direction of the wake.

The auto-correlation of simulated data is in good accordance with experiments for both velocity component at all spanwise locations. This is illustrated by the energy spectrum of u and w shown in Fig. 4 for one of the eight spanwise locations studied. These spectral results indicate that the neural system captures the energy distribution of both signals up to frequencies of 1kHz, i.e., in the frequency range where aliasing errors are negligible. The spatial correlation for the experimental and simulated u velocity component is depicted in Fig. 5. Comparison between the correlation contours in both cases shows that the neural system resolves the flow field well up to a spanwise location $z^*$=-0.2, i.e., up to an extend of five probes, approximately. The auto-correlation functions for the experimental and simulated data, observed along the $x^*$-direction at the top of Figs. 5a and 5b for the extreme probe at location $z^*$=1.2, are also in good agreement. Similar accordance, not shown here for brevity, is found between the spatial correlation of the experimental and simulated w velocity fields.

An estimate of the overall flow structure for the experimental and simulated velocity flow fields is given in Figs. 6 and 7, in terms of the first and second eigenvectors obtained from POD. The neural system adequately describes the flow structure of the turbulent wake flow as indicated by the good agreement observed in these plots between the structures educed from the measured and the predicted velocity fields. The first eigenvector obtained from the simulated two-dimensional velocity field (Fig. 6b) projects to the

one of the real data (Fig. 6a) with a correlation coefficient of 0.97. The neural system identifies the negative fluctuating velocity motions that dominate the wake flow (Ferre-Gine et al. 1996; Kopp et al., 1997), as illustrated by the first eigenvector. This satisfactory description of structure is also observed in the second eigenvector (Figs. 7a and 7b). In this case the neural system also captures the presence of saddle points in the wake flow. In both figures 6 and 7 there is a progressive randomization of the structure for negative $z^*$, consistent with the randomization of the correlation contours presented in Fig. 5.

A pattern recognition analysis carried out to determine the large-scale structural characteristics of the simulated flow shows that 765 windows of 44 instantaneous velocity data with double rollers and 714 windows with saddle points are contained in a simulated time-record of 81600 instants, compared to the 922 and 895 windows of the respective structures present in the experimental data. This 11% reduction in the number of structures present in the simulated data may be due to the inability of the neural system to learn continuity or the three-dimensional characteristics of the structure from two-dimensional information only. It should be mentioned that the proposed neural architecture learned mass conservation when it was applied to a two-dimensional isotropic turbulent velocity field.

The corresponding prototypical patterns or ensemble-averages of the double rollers and saddle points identified by pattern recognition are depicted in Fig. 8 and 9 for both the simulated and experimental velocity fields. The agreement in topology between both vector maps is reasonable, with the saddle point appearing in both cases upstream of the double roller. The correlations between the patterns in Figs. 8a and 8b, and between those in Figs. 9a and 9b are 0.80 and 0.86, respectively. The search for combined double rollers and saddle points yielded similar correlations, which are lower in value than expected from the above POD results but remarkable from the point of view of performance when it is considered that the 2,000 instants of velocity information used for training contains about 22 structures only. These correlations increase to 0.94 when 40,000 instants are used for training, i.e., when the ANN-40000 is used to generate the time-record of 81,600 instants.

A similar performance of the neural system was obtained for data measured along the non-homogeneous vertical plane of the wake ($x^*$-$y^*$). The rake of probes was centered at the wake centerplane $y^*=0$ and spanned vertically the whole wake. In this case, the number of classes contained in the signals measured at the eight different vertical positions depends on the different number of turbulent events sensed by the hot-wires located near the centerplane or near the outer edges of the wake. As a consequence of this dependency on intermittence at least 6,000 instants of the real velocity field (u, v) were needed to train the eight networks, and to capture enough information from the different velocity records so that the generated non-homogeneous turbulent field reproduces the experimental one. It should be noted that the information contained in the vertical plane data is more difficult to learn by the neural system because the coherent structures and associated velocity patterns occurring at the outer edge are different from those at the center region of the wake. In the horizontal plane experiments homogeneity implies that the same type of information is ultimately presented to each individual network.

The architecture proposed is, thus, well fitted to interpret turbulence, as illustrated in the next section, and for real time applications involving turbulent flows. It can also be used to complete time sequences of important data that are limited in size due to difficulties in their acquisition or prediction. For example, the accurate direct numerical simulation of a turbulent flow requires intensive use of CPU time (Kim et al., 1987), which for some flow situations or Reynolds numbers of interest may not be sufficiently available at present. Therefore, the synthetic generation of turbulent velocity or scalar signals or fields with a neural system may be a useful and complementary tool for Computational Fluid Dynamics (CFD).

## INTERPRETATION OF TURBULENCE

To assess the capability of the trained neural system to interpret the large-scale structure of a turbulent velocity field as an expert system it is necessary to study first whether or not the system is capable of generating instantaneous velocity patterns with statistically significant structural features of the flow analyzed, i.e., with features that contribute to the ensemble-average representation of the large-scale structure considered. Fig. 10 depicts the ensemble-average of the instantaneous 900 windows, containing 10 time-sequences of simultaneous velocity data each, that are predicted by the neural system when feeded with 900 input vectors of experimental data extracted from the instantaneous events that contribute to the double roller of Fig. 8b at positions ( $0.4 \leq x^* \leq 1.0$). These input data were not included in the training sets of ANN-2000. Clearly, the structure in Fig. 10 corresponds to the class of large-scale motions represented by the double roller in Fig. 8b. This result indicates that with the same input information as that occurring instantaneously in a laboratory experiment, the neural system generates a group of instantaneous events that yield an ensemble average or prototypical pattern (Fig. 10) that also belongs to the class considered as input (Fig. 8b).

The next step in the evaluation of the neural system as an interactive expert system to help interpreting the structural characteristics of turbulence would be to consider the identification and eduction of coherent structures that could be present in a turbulent flow not previously studied. To simplify this problem it will be assumed here that the unknown turbulent flow is the turbulent wake flow analyzed in the previous section. Thus, the challenge considered is to determine whether the presence of the double roller structure postulated more than fifty years ago from correlation data (Grant, 1958; Payne and Lumley, 1967) exists instantaneously in the flow learned by the neural system. Two interpretation experiments are considered:

(i) Eduction of a double roller with point-to-point forecasting from an sketch of an idealized or assumed template of this structure.

(ii) Testing for double rollers from a single input vector containing the initial portion of the above idealized template.

Figure 11 shows the point to point forecasting from a template of the double roller depicted in Fig. 8b, properly scaled to match the rms values of the fluctuating field considered. This is necessary because the neural system has learned from real examples containing both large-scale and small-scale motions, i.e., from signals of a given amplitude. The predicted velocity map given in Fig. 11 corresponds to a double roller structure centered at $x^*=0$ and with an upstream saddle point at approximately $x^*=1.0$. To support the significance of this finding, several tests of point-to-point forecasting were carried out with input templates of unrealistic or highly improbable vector maps. The results showed that the neural system was unable to converge towards any plausible coherent topology or yield vector maps consistent with the space-time correlation of the data. Note that the velocity vector map of the double roller in Fig. 8b which has been used to generate Fig. 11 does not belong to the training set.

The final test for double rollers is the prediction of an instantaneous vector map of 10 velocity vectors from a properly scaled input vector containing the four instants of information located at $0.8 \leq x^* \leq 1.4$ in Fig. 8b. In this case the neural system predicts the double roller vector map of Fig. 12. There is agreement between the experimental and predicted structures, with the predicted one being slightly smaller in the streamwise direction of the flow. This is probably caused by the difficulty of learning and predicting a three-dimensional phenomena related with the occurrence of ring-shaped vortices (Vernet et al., 1998) from only two-dimensional information. Nevertheless, the remarkable agreement between the double roller structure present in the laboratory data and in the vector map produced by the eight neural networks from information not presented to the networks at the training stage, indicates the potential of the proposed cognitive system to capture the dynamics of turbulent flows. Note that the differences in modulus of the vector plots in both figures are solely caused by the scaling of the input signal.

## CONCLUDING REMARKS

Present results indicate that the proposed neural system is capable of capturing the highly non-linear dynamics of free turbulence. It can also be applied as an interactive expert system in the structural interpretation of turbulence by identifying or recognizing the individual classes of events present in complex shear flows. The present neural architecture based on fuzzy ARTMAP could establish a new trend in the development of systems to control real-time fluid flow phenomena and in the integration of computational and experimental methodologies. It may also become a useful tool in real time optimization procedures for advanced fluid dynamics applications and to complete data banks with sequences of information on complex systems that are limited in extension due to difficulties in the measurement or simulation processes.

## REFERENCES


Adrian, R.J., and Moin, P., 1988, Stochastic estimation of organized turbulent structure: Homogeneous shear flow, Journal of Fluid Mechanics, vol. 190, pp. 531-559.

Antonia, R.A., 1981, Conditional sampling in turbulence measurements, Annual Review of Fluid Mechanics, vol .13, pp. 131-156.

Brown, G.L., and Roshko, A., 1974, On density effects and large structures in turbulent mixing layers, Journal of Fluid Mechanics, vol. 64, pp. 775-816.

Carpenter, G.A., and Grossberg, S., 1987, A massively parallel architecture for a self-organizing pattern recognition machine, Computer Vision, Graphics and Image Processing, vol. 37, pp. 54-115.

Carpenter, G.A., and Grossberg, S. and Reynolds, J.H., 1991[a], ARTMAP: Supervised real-time learning and classification of nonstationary data by a self-organizing neural network, Neural Networks, vol. 4, pp. 565-588.

Carpenter, G.A., and Grossberg, S. and Rosen, D., 1991b, Fuzzy ART: Fast stable learning and categorization of analog patterns by an adaptative resonnace system, Neural Networks, vol. 4, pp. 759-771.

Carpenter, G.A., Grossberg, S., Marcuzon, N., Reinolds, J.H., and Rosen D.B., 1992, Fuzzy ARTMAP: A neural network architecture for incremental supervised learning of analog multidimensional maps, IEEE Transactions on Neural Networks , vol. 3, pp. 698-713.

Denker, J., Schwartz, D., Wittner, B., Solla, S., Howard, R., Jackel, L., and Hopfield, J.J., 1987, Large automatic learning, rule extraction and generalization, Complex Systems, vol. 1, pp. 877-922.

Falco, R.E., 1977, Coherent motion in the outer region of turbulent boundary layers, Physics of Fluids, vol. 20, pp. S124-S132.

Ferre, J.A., and Giralt F., 1989, Pattern recognition analysis of the velocity field in plane turbulent wakes, Journal of Fluid Mechanics, vol. 198, pp. 27-64.

Ferre-Gine, J., Rallo, R., Arenas, A., and Giralt, F., 1996, Identification of coherent structures in turbulent shear flows with a Fuzzy ARTMAP neural network, International Journal of Neural Systems, vol. 7(5), pp. 559-568.

Grant, H.L., 1958, The large eddies of turbulent motion, Journal of Fluid Mechanics, vol. 4, pp. 149-190.

Kadanoff, L.P., 1996, Turbulent excursions, Nature, vol. 382, pp. 116-117.

Kim, J., Moin, P., and Moser, R.J., 1987, Turbulence statistics in fully developed channel flow at low Reynolds number, Journal of Fluid Mechanics, vol. 177, pp. 133-166.

Kopp, G.A., Ferre, J.A., and Giralt, F., 1997, The use of pattern recognition and Proper Orthogonal Decomposition in identifying the structure of fully- developed free turbulence, Journal of Fluids Engineering, vol. 119, pp. 289-296.

Kosko, B., 1992, Neural Networks and Fuzzy Systems , Prentice Hall, Englewood Cliffs. pp. 189-219.

Kühn, R., van Hemmen, J.L., and Riedel, U., 1989, Complex temporal association in neural networks, Journal of Physics A , vol. 22 (15), pp. 3123-3135.

Lee, M., Kim, J., Babcock, D., and Goodman, R., 1997, Application of neural networks to turbulence control for drag reduction, Physics of Fluids, vol. 9, pp. 1740-1747.

Lumley, J.L., 1965, The structure of inhomogeneous turbulent flows, Proceedings of the International Colloquium on Atmospheric Turbulence and Radio Wave Propagation , Moscow, pp. 166-176.

McComb, W.D., 1990, The physics of fluid turbulence, Oxford Univ., Oxford.

Nelkin, M., 1992, In what sense is turbulence an unsolved problem?, Science, vol. 255, pp. 566-569.

Payne, F.R., and Lumley, J.L., 1967, Large eddy structure of the turbulent wake behind a circular cylinder, Physics of Fluids , vol. 10, pp. S194-S196.

Scotti, A., Meneveau, C., and Saddoughi, S.G., 1995, Fractal dimension of velocity signals in high Reynolds-number hydrodynamic turbulence, Physical Review E, vol. 51, pp. 5594-5608.

Seung, H.S., Sompolinsky, H., and Tishby, N., 1992, Statistical mechanics of learning from examples , Physical Review A, vol. 45, pp. 6056-6091.

Sreenivasan, K.R., 1990, Fluid dynamics turbulence and the tube, Nature, vol. 344, pp. 192-193.

Takens, F., 1981, Detecting strange attractors in turbulence, Dynamical systems and turbulence, Lecture Notes in Mathematics, vol. 898, pp. 366-381.

Tzes, A., and Borowiec, J., 1996, Applications of fuzzy logic and neural networks to identification and control problems in fluid mechanics, Proceedings of ASME Fluids Engineering Division, FED-242, pp. 29-34.

Townsend, A.A., 1976, The structure of turbulent shear flow, 2n Edition, Cambridge Univ., Cambridge.

Vernet, A., Kopp, G.A., Ferre, J.A., and Giralt, F., 1998, Three-dimensional structure and momentum transfer in a turbulent cylinder wake, Journal of Fluid Mechanics , submitted.

Zadeh, L., 1965, Fuzzy sets, Information and Control , vol. 8, pp. 338-353.

**Table 1**

Statistics of the experimental and simulated data with velocities in m/s.

| | Experimental | | | ANN-2000 | | | ANN-24000 | | |
|---|---|---|---|---|---|---|---|---|---|
| | mean | rms | uw | mean | rms | uw | mean | rms | uw |
| $u_1$ | 0.000 | 0.118 | | 0.010 | 0.119 | | 0.008 | 0.114 | |
| $w_1$ | 0.000 | 0.087 | 0.001 | -0.002 | 0.083 | 0.001 | -0.001 | 0.081 | 0.001 |
| $u_2$ | 0.000 | 0.117 | | 0.012 | 0.109 | | 0.004 | 0.108 | |
| $w_2$ | 0.000 | 0.087 | 0.002 | 0.000 | 0.087 | 0.001 | 0.001 | 0.079 | 0.001 |
| $u_3$ | 0.000 | 0.118 | | 0.012 | 0.113 | | 0.003 | 0.110 | |
| $w_3$ | 0.000 | 0.087 | 0.000 | 0.001 | 0.080 | 0.000 | -0.001 | 0.079 | 0.000 |
| $u_4$ | 0.000 | 0.117 | | 0.016 | 0.109 | | 0.006 | 0.110 | |
| $w_4$ | 0.000 | 0.087 | 0.000 | -0.003 | 0.082 | 0.000 | 0.000 | 0.078 | 0.000 |
| $u_5$ | 0.000 | 0.120 | | 0.009 | 0.109 | | 0.004 | 0.113 | |
| $w_5$ | 0.000 | 0.088 | 0.001 | 0.003 | 0.086 | 0.001 | 0.002 | 0.081 | 0.001 |
| $u_6$ | 0.000 | 0.117 | | 0.011 | 0.110 | | 0.007 | 0.115 | |
| $w_6$ | 0.000 | 0.088 | 0.000 | 0.011 | 0.085 | 0.000 | 0.003 | 0.077 | 0.001 |
| $u_7$ | 0.000 | 0.120 | | 0.010 | 0.120 | | 0.005 | 0.117 | |
| $w_7$ | 0.000 | 0.087 | -0.001 | 0.007 | 0.082 | -0.001 | 0.001 | 0.080 | 0.000 |
| $u_8$ | 0.000 | 0.111 | | -0.007 | 0.108 | | 0.002 | 0.106 | |
| $w_8$ | 0.000 | 0.084 | -0.002 | -0.005 | 0.083 | -0.002 | -0.002 | 0.079 | -0.001 |

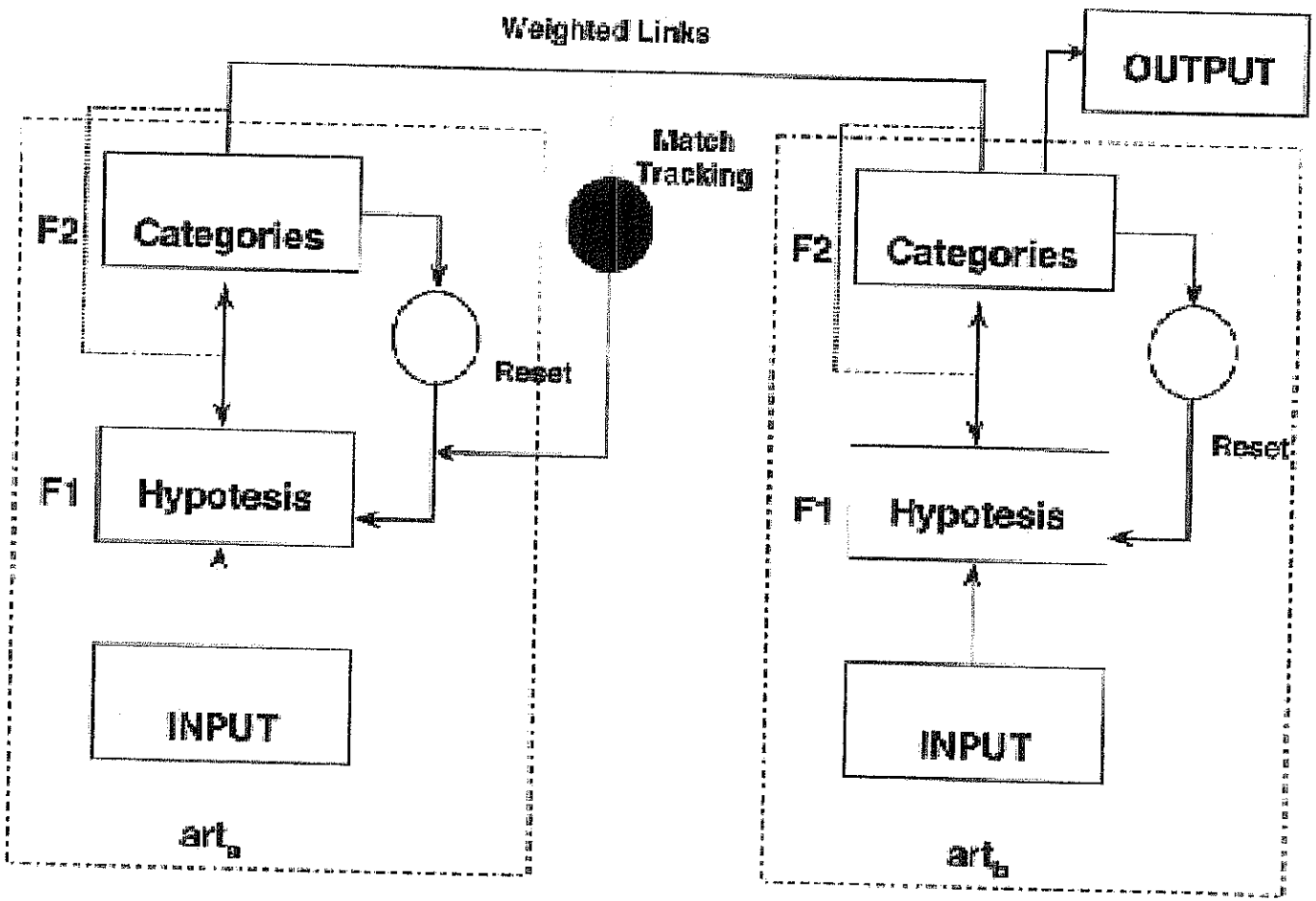


1. Individual neural network architecture

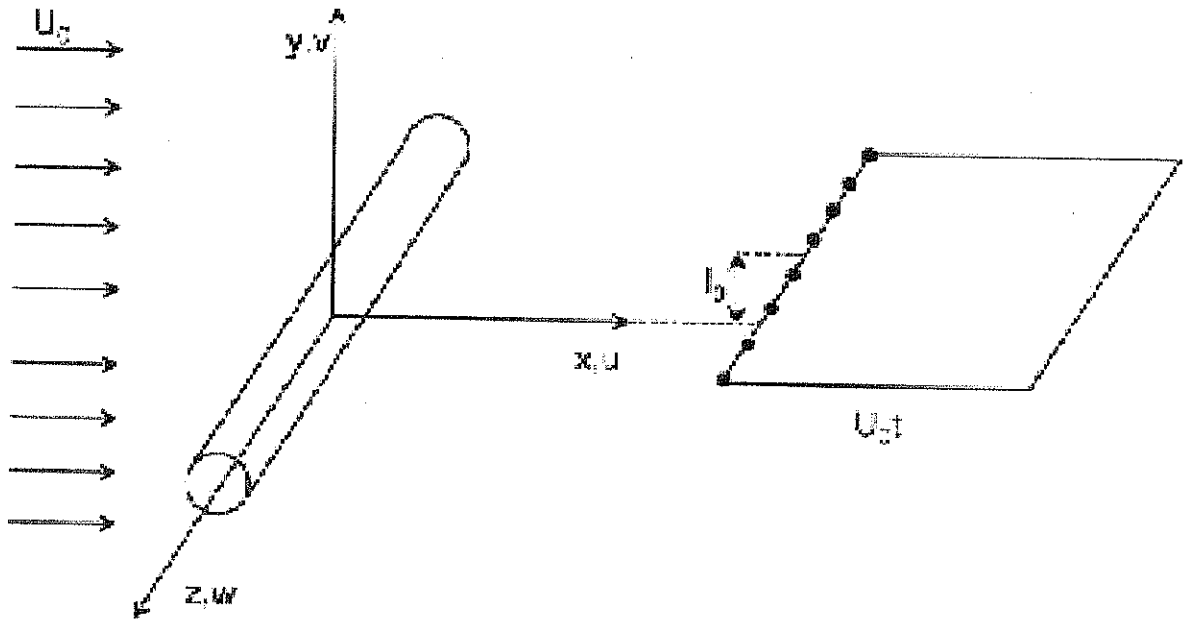


2. Sketch of the flow configuration

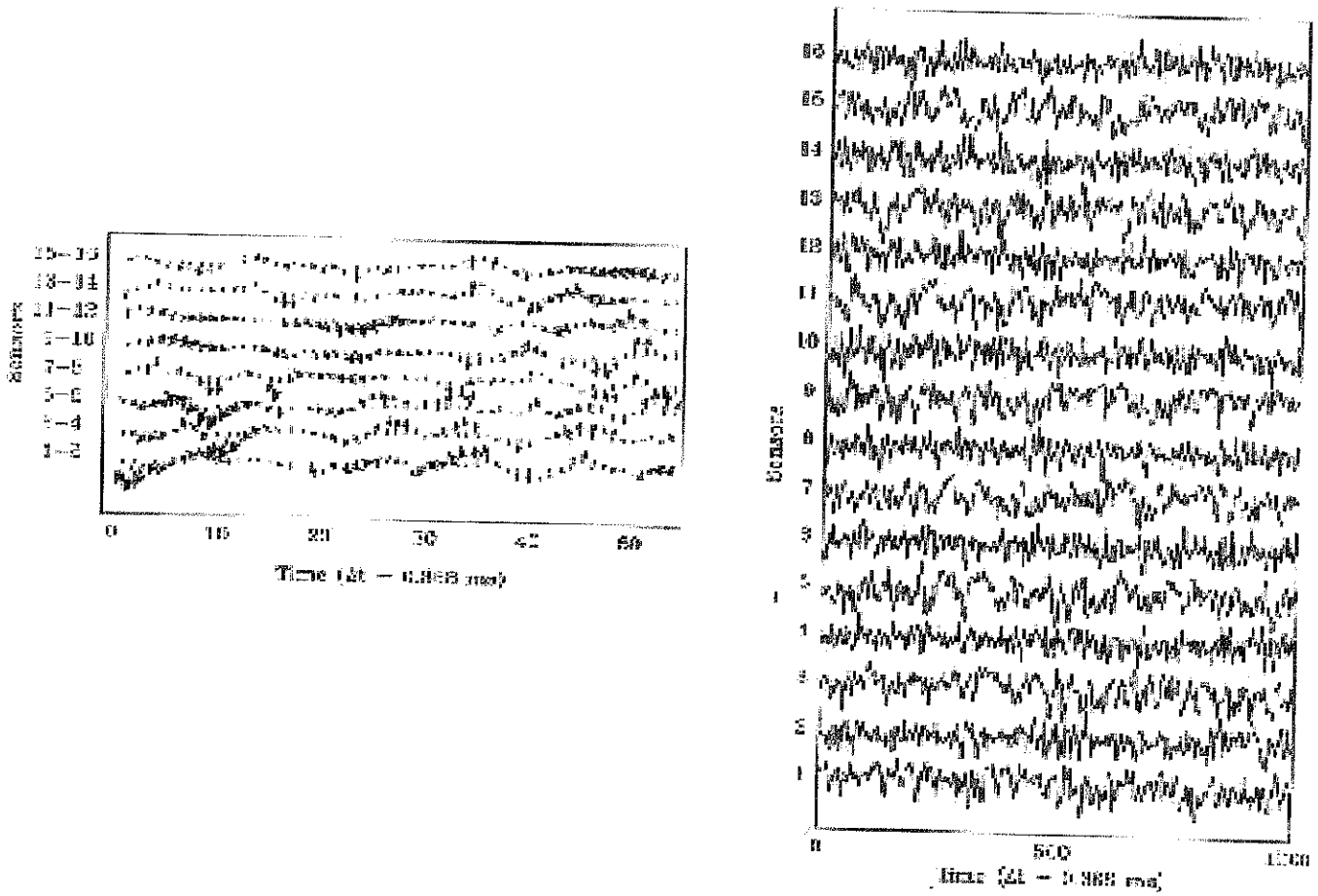

3. Sample of $(x,w)$ experimental data. The time interval between two consecutive samples points is $\Delta t = 0.368$ ms.

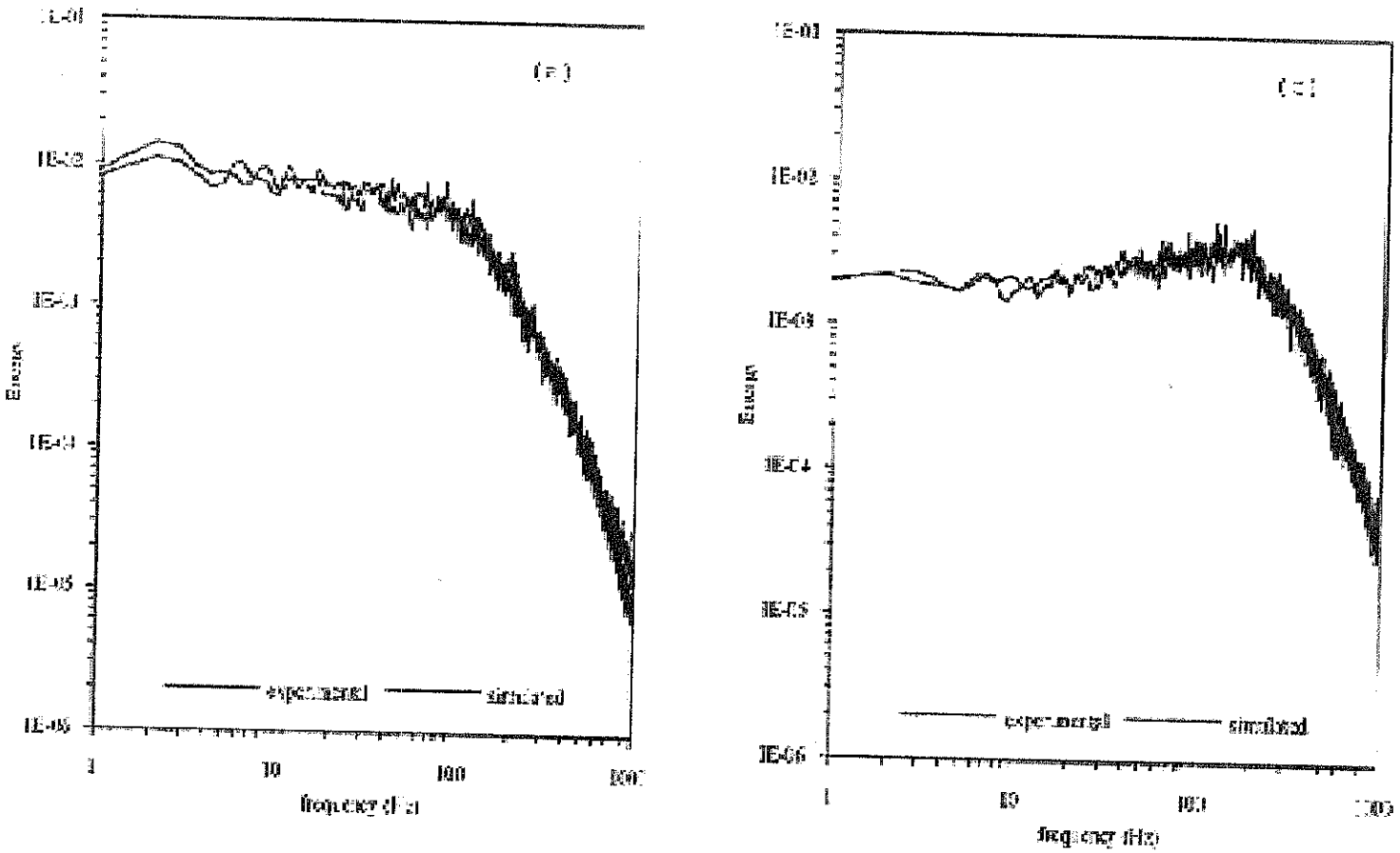


4 Autospectra of the (a) streamwise and (c) spanwise velocity

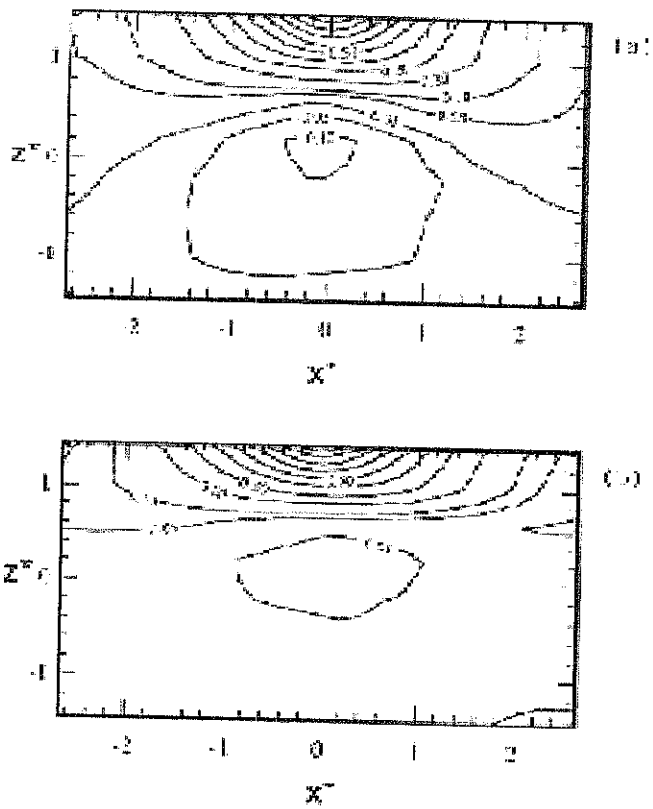

5. Circulation of the streamwise velocity field.

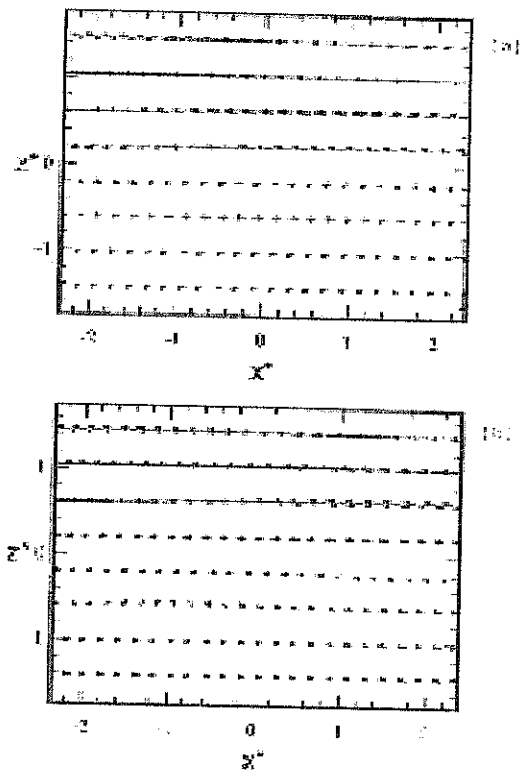

8. First eigenvector from the POD analysis of the (a) experimental and (b) simulated data.

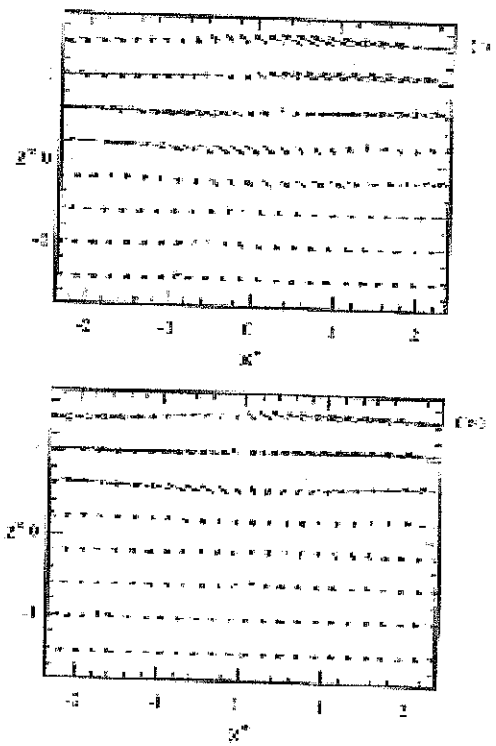

7. Second eigenvector from the POD analyses of the (a) experimental and (b) simulated data.

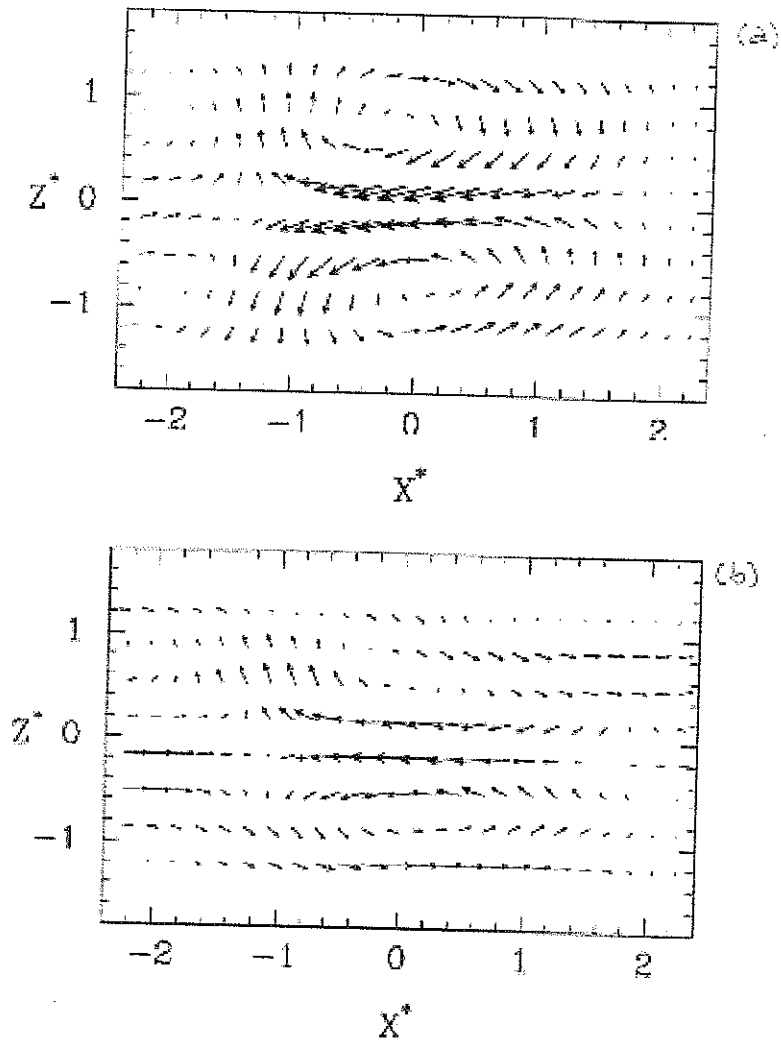


8. Pattern recognition analyses of double rollers: (a) experimental and (b) simulated data.

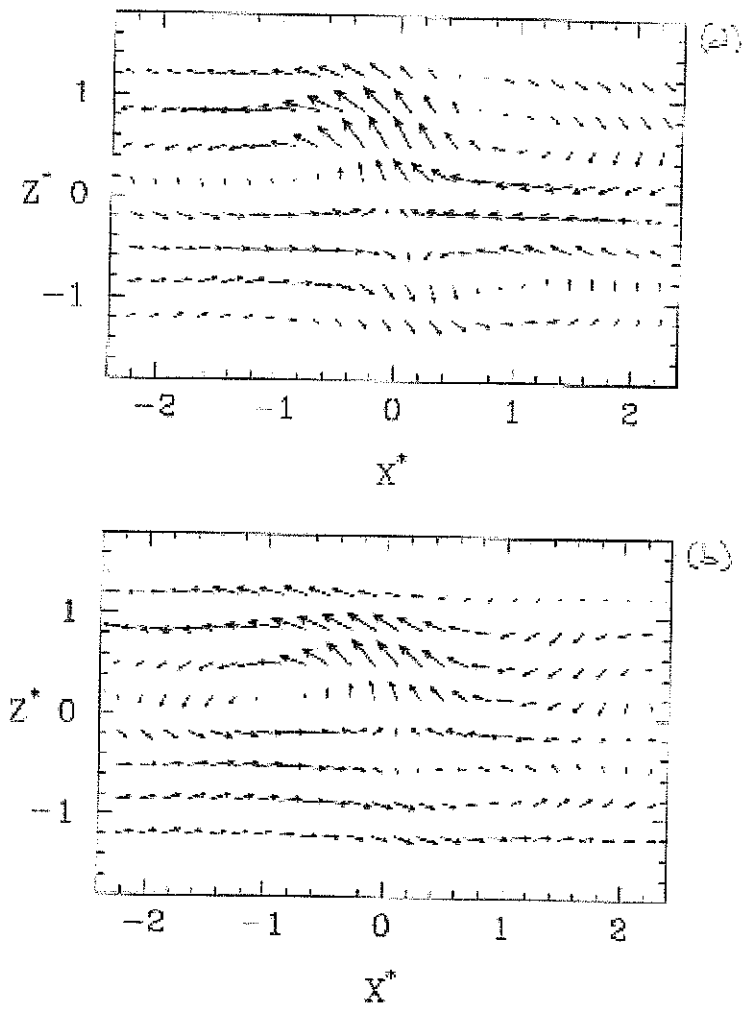


9. Pattern Recognition analyses of saddle points: (a) experimental and (b) simulated data.

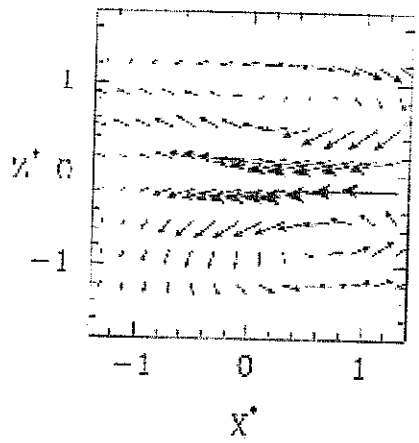


10. Ensemble average of vectors maps predicted by the neural system when feeded with input vectors of experimental data extracted from the instantaneous events that contribute to the double roller of Fig. 8h at positions $0.4 \leq x^* \leq 1.0$.

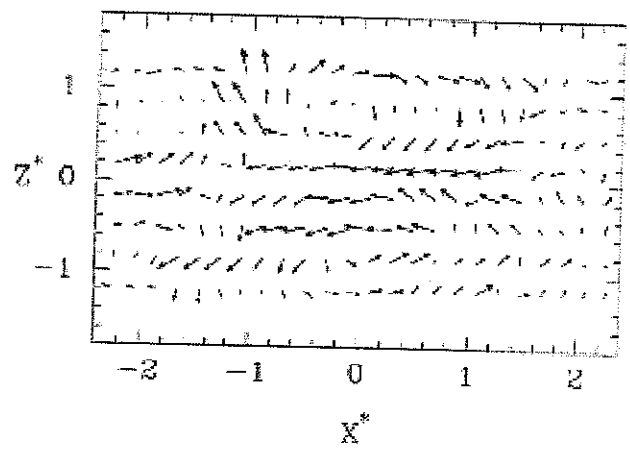


11. Point-to-point forecasting of a vector map from an idealized and scaled double roller template.

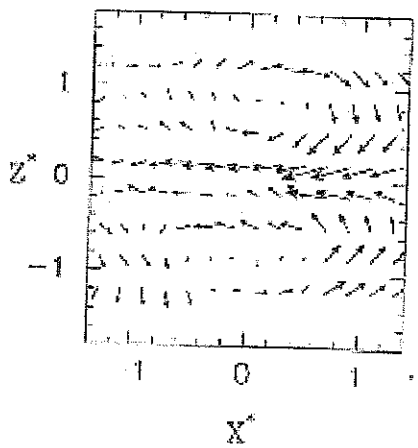


12. Prediction of an instantaneous vector map from an idealized and scaled double roller template.